Research article

Performance assessment of a solar powered hydrogen production system and its ANFIS model

S. Senthilraja [a,*], R. Gangadevi [a], Hasan Köten [b], R. Marimuthu [c]

[a] Department of Mechatronics Engineering, SRM Institute of Science and Technology, India
[b] Department of Mechanical Engineering, Istanbul Medeniyet University, Istanbul, Turkey
[c] Department of Electrical and Electronics Engineering, Vellore Institute of Technology, India

ARTICLE INFO

ABSTRACT

Apart from many limitations, the usage of hydrogen in different day-to-day applications have been increasing drastically in recent years. However, numerous techniques available to produce hydrogen, electrolysis of water is one of the simplest and cost-effective hydrogen production techniques. In this method, water is split into hydrogen and oxygen by using external electric current. In this research, a novel hydrogen production system incorporated with Photovoltaic – Thermal (PVT) solar collector is developed. The influence of different parameters like solar collector tilt angle, thermal collector design and type of heat transfer fluid on the performance of PVT system and hydrogen production system are also discussed. Finally, thermal efficiency, electrical efficiency, and hydrogen production rate have been predicted by using the Adaptive Neuro-Fuzzy Inference System (ANFIS) technique. Based on this study results, it can be inferred that the solar collector tilt angle plays a significant role to improve the performance of the electrical and thermal performance of PVT solar system and Hydrogen yield rate. On the other side, the spiral-shaped thermal collector with water exhibited better end result than the other hydrogen production systems. The predicted results ANFIS techniques represent an excellent agreement with the experimental results. In consequence, it is suggested that the developed ANFIS model can be adopted for further studies to predict the performance of the hydrogen production system.

1. Introduction

The continuous usage and depletion of petrol, diesel and CNG etc., and increase the vehicle population gives more threat to the environment (Hites, 2006). In addition, the uncertainty in crude oil price and increasing of exhaust emissions caused by vehicles and industries, it is utmost importance to find the suitable fuel to replace the crude based fuels. Among other fuels, because of high conversion efficiency and clean in nature, the using of hydrogen as a primary or secondary fuel in different applications is increasing dramatically in recent years (Ambrose et al., 2017; Ahmadi and Kjeang, 2015; Larsson et al., 2015; Lipman et al., 2018; Gadalla and Zafar, 2016). Generally, hydrogen is not available in nature like crude oil. However, different techniques such as natural gas steam reforming, coal gasification and water electrolysis etc. adopted to produce hydrogen, water electrolysis is one of the simplest and cheapest technique (Chen et al., 2008; Ersöz, 2008; Balthasar, 1984; Bamberger and Richardson, 1976). In this electrolysis process, water is split into Hydrogen (H_2) and Oxygen (O_2) by using external direct current

(Rossmeisl et al., 2005). Generally, the electrolyzer setup consists of fluid container with two electrodes such as anode and cathode. These two electrodes are immersed in water and connected to the external power supply. While supplying external power to the electrodes, the water is split into hydrogen and oxygen and the hydrogen is obtained from the cathode. The general chemical reaction happens during the electrolysis process is given below

$$2H_2O \rightarrow 2H_2 + O_2 \tag{1}$$

At the same time, numerous systems have been developed by utilizing the solar energy. Though the photovoltaic (PV) based systems possess few limitations, because of many advantages, solar energy based systems are inevitable in recent years. Photovoltaic system converts partial solar radiation into electrical energy and the remaining solar radiation is converted into heat. This unwanted heat directly affects the electrical output of the Photovoltaic system. Hence, the continuous research is going on to increase the electrical output of the PV system by reducing its temperature. Combining different shaped thermal collector with PV
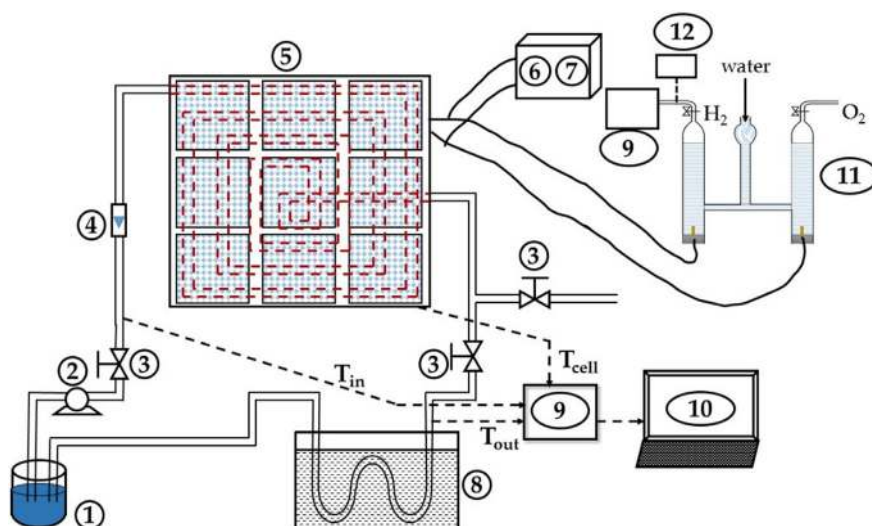

Figure 1. Schematic of PVT based hydrogen production system. 1 – Collecting tank, 2 – Pump, 3 – Flow control valve, 4 – Flow meter, 5 – PVT solar collector, 6 – Voltmeter, 7 – Ammeter, 8 – Heat exchanger unit, 9 – Hydrogen storage tank, 10 – Personal computer, 11 – Hoffman Voltameter, 12 – Flow sensor.

module is one of the simplest and feasible method to enhance the electrical power output. This system is named as 'Photovoltaic – Thermal (PVT)' solar collector (or) 'Hybrid solar collector'. In the past few years, different heat transfer fluids such as water, air and Ethylene Glycol (EG) are mainly used in thermal collector to extract the heat from PV module.

Tiwari et al. have analyzed the performance of PVT/air solar collector based dryer and found 26.68% of thermal efficiency, 11.26% of electrical efficiency and 56.3% of overall efficiency at constant mass flow rate of 0.01 kg/s (Tiwari et al., 2018). Hegazy has attempted to develop a drying system incorporated with air based PVT system (Hegazy, 2000). This study was carried out by passing the air in single time and double time. Fudholi et al. have carried out experimental and theoretical studies to investigate the exergy and sustainability index of PVT/air solar collector (Fudholi et al., 2019). The exergy efficiency of 13.36% and 12.89% was achieved by means of experimental and theoretical studies respectively. Similarly, sustainability index of 1.168 and 1.148 was achieved by experimental and theoretical studies respectively. Bambrook and Sproul (2016), Farshchimonfared (Farshchimonfared et al., 2015) and Touafek (Touafek et al., 2018) studied the performance of PVT solar collector with air as medium of heat transfer fluid.

Thermal collectors efficiency relied on the thermal properties of the heat transfer fluid. Since the air possess poor heat transfer characteristics when compared to water, many researchers have studied the PVT solar collector with water. Yazdanpanahi et al. (2015), Aste et al., 2015, 2017, Tiwari et al. (2016) and Rawat and Dhiran (2017) investigated the performance of water based PVT solar collector by varying different operating parameters. With the above literatures, it has been inferred that the temperature of PV module has been reduced significantly. Hence, the thermal, electrical and overall efficiencies of the PVT solar collector also increased reasonably with water and air. The performance of PVT solar collector not only depends on the heat transfer fluids but also mainly depends on other factors such as tilt angle, wind velocity, solar radiation and photovoltaic cell materials etc. Le Roux (Le Roux, 2016), Jain and Lalwani (2017), Myhan et al. (2017), Bracamonte et al. (2015), Gökmen et al. (2016) and Lu and Zhao (2018) studied the performance of photovoltaic solar collectors with different operating conditions. Because of these positive results, the research on the development of solar energy based hydrogen production system is increased rapidly in recent years (Chi and Yu, 2018; Jia et al., 2016; Bhattacharyya et al., 2017; Dahbi et al., 2016; Li, 2017).

From these literature results, it is observed that the efficiency of the conventional fuel based systems can be improved by replacing with hydrogen. Till now, many researchers have developed and analyzed the

hydrogen production system powered by solar energy. Nevertheless, very few researchers used PVT solar collectors to produce the hydrogen and published their results in different articles. Hence, this research is mainly focused to study the impact of PV module tilt angle, solar collector design and heat transfer fluid on the performance of PVT solar collector and hydrogen yield rate of PVT based hydrogen production system. In this work, the test has been conducted with three different tilt angles (i.e. 30°, 40° and 50°) and two types of thermal collectors (Spiral shape and Oscillatory flow). Also in this study, water, Ethylene Glycol and water - Ethylene Glycol Mixture are used as heat transfer fluids. At the outset, these experimental results have been validated by using Adaptive Neuro Fuzzy Inference (ANFIS) techniques.

2. Experimental setup and methodology

The experiments have been conducted on an electrolysis setup along with photovoltaic – Thermal collector, temperature sensors, flow meter, pyranometer, pump and multi-channel data acquisition systems. The schematic of the fabricated experimental setup is presented in Figure 1. The heat transfer fluid is circulated into the PVT system by using centrifugal pump. The flow rate is connected at the outlet side of the pump and measured the flow rate of the fluid. The spiral and oscillatory flow thermal collectors are made with 12.7mm outside diameter and 10.26 mm inner diameter copper tube and fixed with the PV module. However, the temperature of the heat transfer fluid is reduced by using the heat exchanger unit before goes to the collecting tank. The voltage, current and temperature values are noted with the help of indicators available in the control panel. The personal computer installed with the LabVIEW software is used to store the values for further calculations.

2.1. Experimental procedure

As per the schematic diagram given in Figure 1, the test setup is fabricated and tests are carried out with different operating conditions. To measure the hydrogen yield rate and electrical efficiency of PVT system, the top surface of the PV module is placed towards South direction at three different angles (i.e. 30°, 40° and 50°). At each angle, different output parameters such as PV module surface temperature, inlet and outlet fluid temperature, open circuit voltage and short circuit current are continuously measured by the circulating water, Ethylene Glycol and water - Ethylene Glycol mixture in the thermal collector. The same test is repeated continuously for seven days and the average values are considered for further calculations.

Table 1. List of measuring instruments and its uncertainty.

Equipment with model No	Parameter	Accuracy	Uncertainty
Solar power meter (TM-207)	Irradiance	$\pm 10 W/m^2$	$\pm 1.3\%$
Digital multi meter (DT830D)	short circuit current	$\pm(1.0\% + 5)A$	± 0.03
Digital multi meter (DT830D)	open circuit voltage	$\pm(0.5\% + 3)V$	± 0.05
Thin film RTD Thermocouples	PV surface temperature	$\pm 0.14\,°C$	$0.14\,°C$
K type Thermocouple	collector inlet, outlet, and ambient temperature	$\pm 1.09\,°C$	$\pm 0.09\,°C$
Flow meter (kg/s)	Flow rate	± 0.22	± 0.20

3. Data reduction

The overall efficiency of the PVT solar collector can be calculated by adding thermal efficiency with electrical efficiency. The overall efficiency equation for the PVT solar collector can be written as

$$\eta_{overall} = \eta_{thermal} + \eta_{electrical} \tag{2}$$

$$\eta_{overall} = \left[\frac{\mathring{m}\, C_p\,(T_{out} - T_{in})}{A_C\, G_T}\right] + \left[\frac{V_{OC}\, I_{SC}\, FF}{A_P\, G_T}\right] \tag{3}$$

Where $\mathring{m}$, C_p, G_T, A_C and A_P are the mass flow rate of fluid (kg/s), specific heat of fluid (J/kg K), total solar radiation (W/m^2) and area of thermal collector and photovoltaic module (m^2) respectively. Similarly V_{OC}, I_{SC} and FF are the open circuit voltage (Volts), short circuit current (Amps) and fill factor (0.7) respectively. The temperature of inlet and outlet fluid temperatures are denoted as T_{in} and T_{out} respectively.

The volume of hydrogen produced in this study can be computed as

$$V_{H_2} = \frac{R\, I_{el}\, T_a\, t}{F\, P\, Z} \tag{4}$$

Where R, I_{el}, T_a and t are the gas constant (8.314 J/mol. K), input current to electrolyzer (Amps), Atmosphere temperature (K) and current supplied duration (sec). Also, the Faraday constant (96485.3 C/mol), Atmosphere pressure (1.01325×10^5 N/m^2) and number of excess electrons (2 for Hydrogen) are denoted as F, P and Z respectively.

4. Uncertainty analysis

During this study, the performance of PVT system has been studied by measuring different parameters in the system. Therefore, the uncertainty of the PVT system relies on the uncertainty of every measuring in-struments. The following equation can be used to compute the uncertainty error of the PVT system.

$$eR = \left[\left(\frac{\partial R}{\partial V_1}e_1\right)^2 + \left(\frac{\partial R}{\partial V_2}e_2\right)^2 + \ ..... \ + \left(\frac{\partial R}{\partial V_n}e_n\right)^2\right]^{0.5} \tag{5}$$

where 'eR' is over all uncertainty, 'R' is objective of separate variable R = R (V$_1$,V$_2$, … V$_n$), e$_i$- uncertainty interval in the nth variable and $(\partial R/\partial V)$. By using the above equation, the uncertainty of individual instruments measured and given in Table 1. From this, the overall uncertainty error is calculated and it is found to be less than $\pm 2\%$

$$eR = \left[(1.3)^2 + (0.03)^2 + (0.05)^2 + (0.14)^2 + (0.09)^2 + (0.2)^2\right]^{0.5} = \pm 1.32 \tag{6}$$

5. Result and discussion

A novel system incorporated with PVT system that generates hydrogen has been developed and investigated for its performances. During this study, the incident solar radiation is considered as 700 W/m^2 and the different parameters such as PV module inclination angle (i.e. 30°, 40° and 50°), heat transfer fluids (water (W), Ethylene Glycol (EG) and Water + Ethylene Glycol (W + EG)) and thermal collector design (Spiral Collector (SC) and Oscillatory Flow (OF)) are changed.

As the time increases from 8.00 to 12.00, the thermal efficiency of all solar collectors increased afterwards decreased till the day end (See Figure 2). These figures clearly shows that the thermal output increases with increasing the tilt angle and the optimum tilt angle is observed as 40°. When the PV module is placed at 30° inclination angle with the horizontal plane, less amount of sun light falls on the PV module and more amount of incident solar energy reflected into the atmosphere at 50°. Hence the PVT module with 40° inclination angle produces more
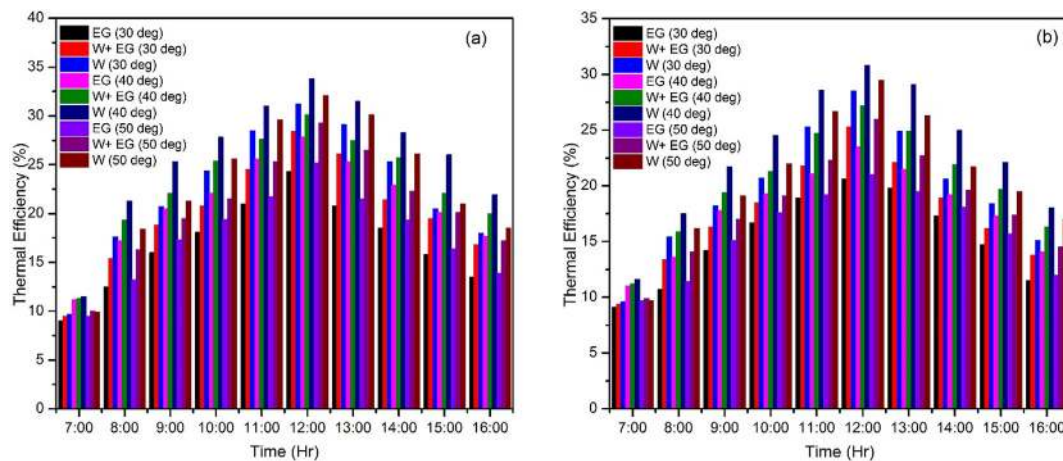

Figure 2. Effect of inclination angle and heat transfer fluids on thermal efficiency of PVT solar collector with (a) Spiral flow thermal collector (b) Oscillatory flow thermal collector.
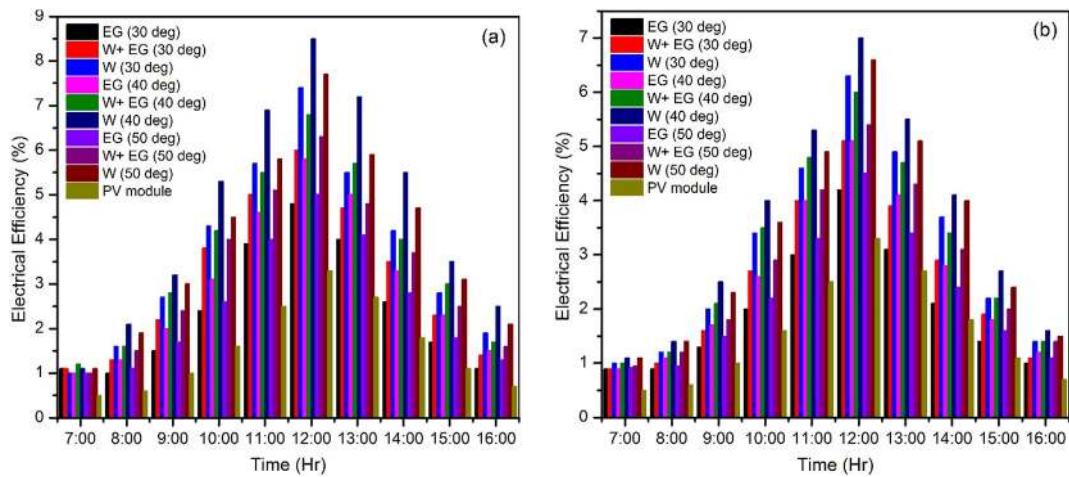
Figure 3. Effect of inclination angle and heat transfer fluids on electrical efficiency of PVT solar collector with (a) Spiral flow thermal collector (b) Oscillatory flow thermal collector.
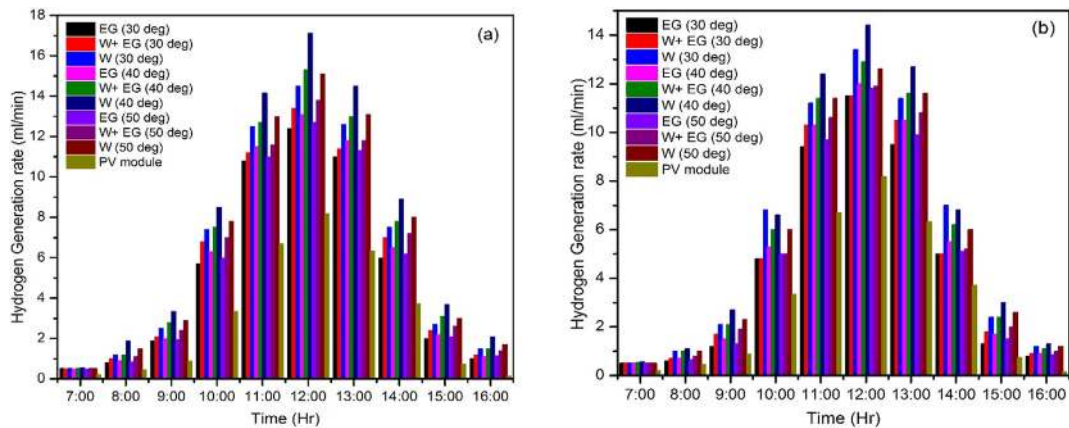

Figure 4. Effect of inclination angle and heat transfer fluids on Hydrogen yield rate with (a) Spiral flow thermal collector (b) Oscillatory flow thermal collector.

thermal output compared with other PVT systems. On the other hand, the water possess more heat transfer characteristics compared with Ethylene Glycol and time taken by fluid in spiral flow thermal collector is more compared with the oscillatory flow type. This is the possible reason to achieve more thermal output for the water based spiral flow type PVT system with 40̂inclination angle.

According to these figures, at 12.00, the higher amount of thermal efficiency of 33.8% have been obtained with spiral flow PVT system cooled with water placed at an angle of 40° inclination. Whereas for 30° and 50° inclination angles the observed values are 31.2% and 32.1% respectively. At the same operating conditions, the values decreased to 30.1%, 28.4% and 29.3% respectively for oscillatory flow type PVT system with water. Furthermore, a slight decrease in thermal efficiency have also been noticed for PVT systems cooled with Ethylene glycol, water and Ethylene Glycol mixture.

Electrical output of spiral flow and oscillatory flow PVT systems cooled at various inclination angles with different heat transfer fluids are presented in Figure 3. The electrical output gets higher while using the spiral flow type PVT system cooled with water at 40° inclination angle with the horizontal plane. The electrical output slightly get decreased for oscillatory flow when compared to the spiral flow type. At all times, the lowest electrical output is observed for oscillatory flow type PVT system with ethylene glycol at 30° inclination angle. As the inclination angle increased to 40°, the electrical output also increased then it drops when the inclination angle goes up. On the other hand, with all heat transfer fluids, the spiral flow type PVT system converts more heat into electrical

energy compared to oscillatory type. According to these results, at 12.00, the lowest electrical efficiency of the oscillatory PVT system cooled with Ethylene Glycol inclined at 30°, 40° and 50° were as 4.2%, 5.1% and 4.5% respectively. In the case of spiral flow type the values increased to 4.8%, 5.8% and 5% respectively. Further, for the oscillatory and spiral flow PVT system with water, the maximum electrical efficiency values were found as 6.3%, 7% and 6.6% and 7.4%, 8.5% and 7.7% respectively.

Comparing the PVT system with spiral flow type against the oscillatory flow, spiral flow thermal collector has a more fluid and PV module surface contact and more convection heat transfer took place at all inclination angles which leads to decrease the PV module temperature significantly. On the other hand more amount of solar radiation absorbed by the PV module, when the PV module is placed at 40° inclination angle. These are the possible reasons to observe more electrical efficiency for spiral flow PVT system cooled with water at 40° inclination angle.

Figure 4 presents the influence of tilt angle, thermal collector design and heat transfer fluids on hydrogen generation rates. It can be realized from these figures that the use of spiral flow thermal collector with water at 40° inclination angle improved hydrogen generation rates compared to other systems.

While using Ethylene Glycol in spiral flow PVT system at 30°, 40° and 50° inclination angles, the peak hydrogen generation rates were found as 12.4 ml/min, 13.1 ml/min and 12.7 ml/min respectively. The values slightly decreased to 11 ml/min, 12 ml/min and 11.8 ml/min respectively for oscillatory flow system. Whereas for water based spiral flow system at 40°, the hydrogen generation rate had a variation from 0.56
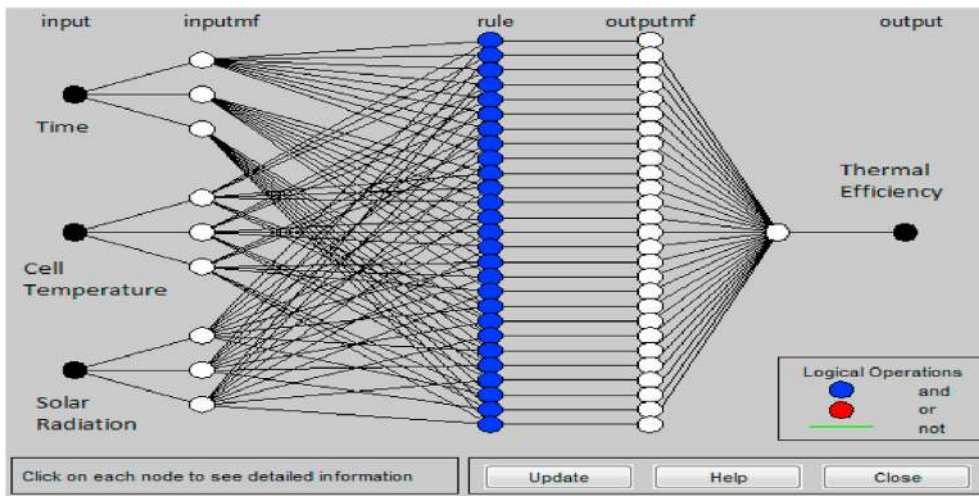
Figure 5. Architecture of ANFIS with input and output parameters.

ml/min to 17.12 ml/min when the time varies from 7.00 to 12.00, then it decreased to 2.1 ml/min at 16.00. Maximum energy conversion and heat transfer in PV module during the operation is expected in water based PVT system at 40° inclination angle. This tends to produce more electrical output in the PV module. This accelerates the electrolysis process in electrolyzer. Due to these facts that the hydrogen generation rate increased gradually from 7.00 to 12.00 then it drops till the day end for all systems and generates more hydrogen at 12.00.

6. ANFIS

Though the practical systems are simple in construction but consumes more time to obtain the final result. Hence, the mathematical representation of the practical systems are very important to analyze the system performance very quickly. After the invention of high speed computers, many artificial intelligence techniques such as Neural Network (Samara and Natsheh, 2018; Batayneh et al., 2020; Awolusi et al., 2019), Fuzzy logic (Rivera-Niquepa et al., 2020) have been increased to find the relationship between the input and output. In the nineteenth century (i.e.

1995) Jang and Sun developed and proposed an intelligent hybrid system called as Adaptive Neuro Fuzzy Inference System (ANFIS) by combining Artificial Neural network (ANN) with Fuzzy system (Jang and Sun, 1995). Generally, fuzzy system comprises IF - Then rules, membership functions and an inference system. Fuzzy rules and membership functions are determined by using ANN. From the name, it can be understood that the fuzzy membership tuned automatically based on the environment. Therefore, the ANFIS gives better learning ability with less percentage error. Generally, Sugeno is one of the most famous model. Thus this present study is based on the Sugeno – Fuzzy inference system. This system is described with the help of two inputs, two fuzzy If- Then rules and one output (Brown, 1994). This consists of two fuzzy sets (A and B) and determining parameters during training (p,q and r)

Rule 1: If (x1 is A1) and (x2 is B1) then $f_1 = p_1x_1 + q_1x_2 + r_1$ (7)

Rule 2: If (x1 is A2) and (x2 is B2) then $f_2 = p_2x_1 + q_2x_2 + r_2$ (8)

The general architecture of ANFIS is given in Figure 5 and described as follows. As shown in Figure 5 inputs such as Time, Cell temperature
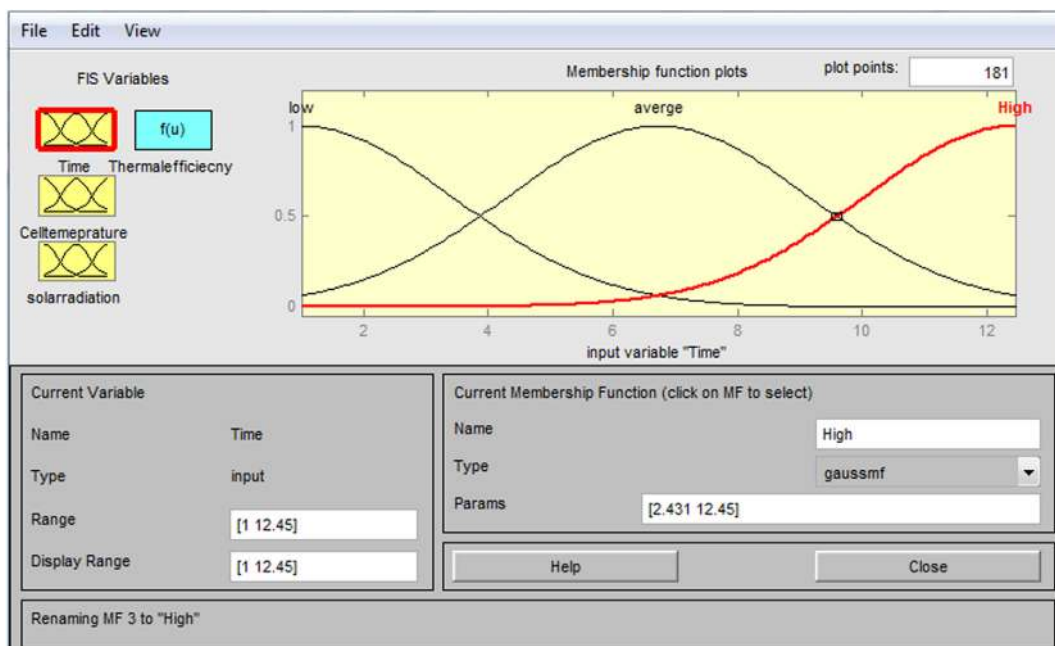

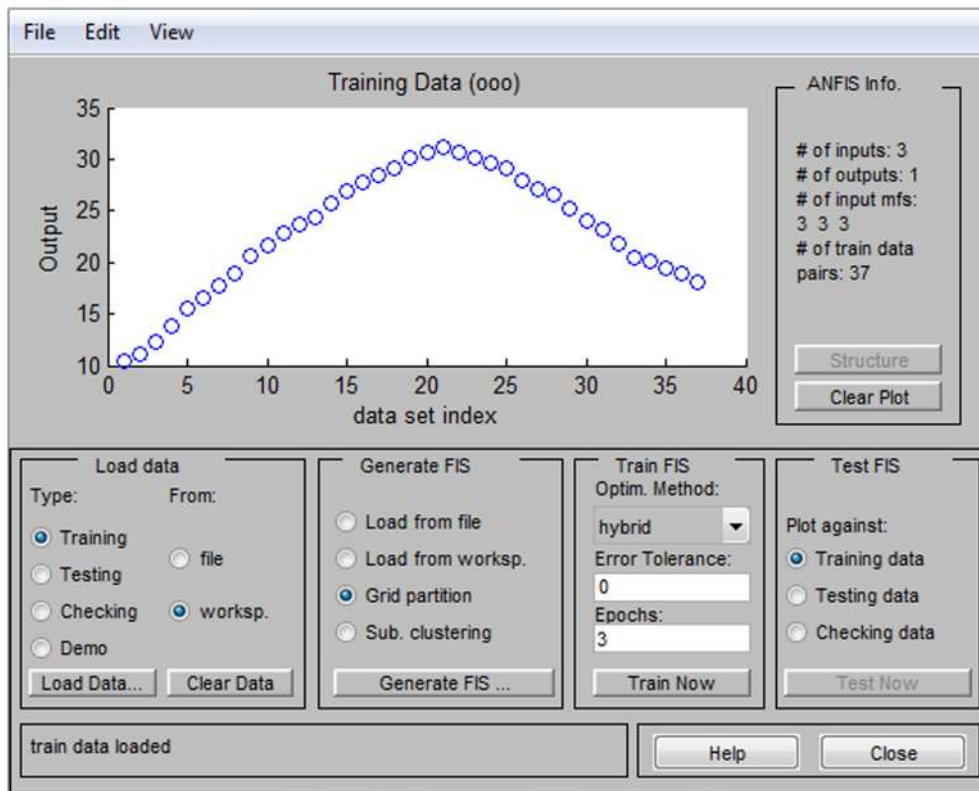**Figure 6.** Membership function with three linguistic variables.
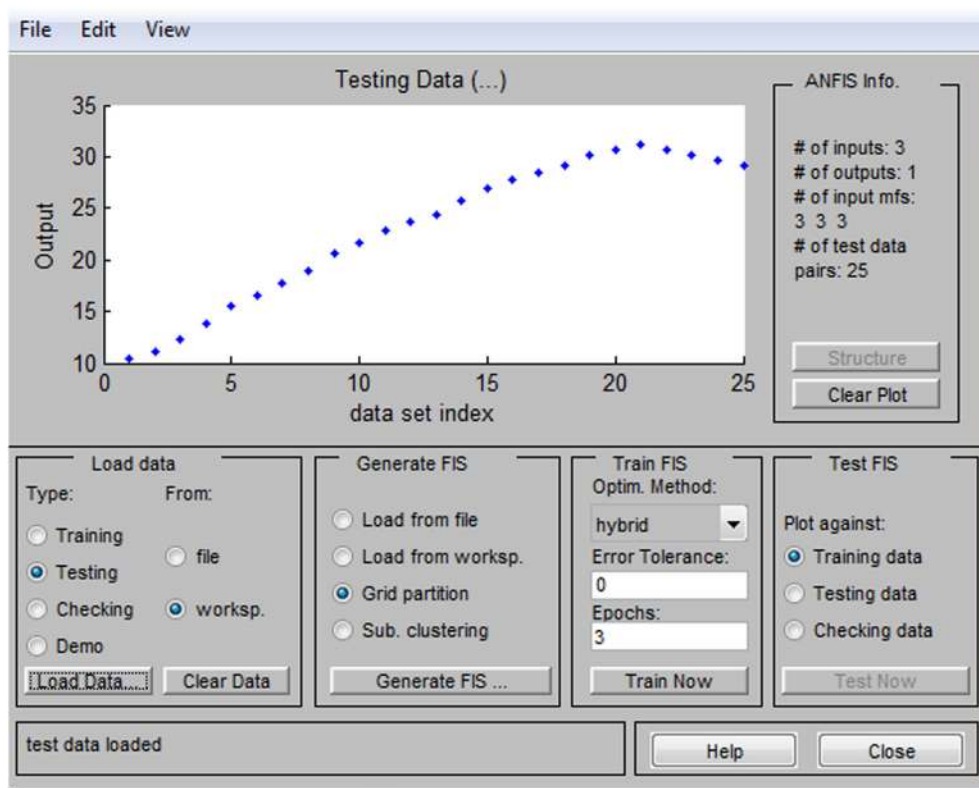
Figure 7. Loading of training data set.

Figure 8. Loading of testing data set.

Table 2. Statistical parameters for input and target data.

	Input		Target		
	Cell Temperature (°C)	Radiation (W/m²)	Thermal Efficiency (%)	Electrical Efficiency (%)	Hydrogen Yield rate (ml/min)
Minimum	34.1	421	10.5	1	0.53
Maximum	39.2	935	31.2	7.4	14.5
Average	36.63	664.297	23.041	3.877	6.701
Standard Deviation	1.3868	176.1856	5.9136	1.8833	4.9350

Table 3. Linguistic rules.

Rule Number	Rule
1	If (Time is low) and (Celltemeprature is low) and (solarradiation is low) then (Thermalefficiecny is out1mf1) (1)
2	If (Time is low) and (Celltemeprature is low) and (solarradiation is average) then (Thermalefficiecny is out1mf2) (1)
3	If (Time is low) and (Celltemeprature is low) and (solarradiation is high) then (Thermalefficiecny is out1mf3) (1)
4	If (Time is low) and (Celltemeprature is average) and (solarradiation is low) then (Thermalefficiecny is out1mf4) (1)
5	If (Time is low) and (Celltemeprature is average) and (solarradiation is average) then (Thermalefficiecny is out1mf5) (1)
6	If (Time is low) and (Celltemeprature is average) and (solarradiation is high) then (Thermalefficiecny is out1mf6) (1)
7	If (Time is low) and (Celltemeprature is High) and (solarradiation is low) then (Thermalefficiecny is out1mf7) (1)
8	If (Time is low) and (Celltemeprature is High) and (solarradiation is average) then (Thermalefficiecny is out1mf8) (1)
9	If (Time is low) and (Celltemeprature is High) and (solarradiation is high) then (Thermalefficiecny is out1mf9) (1)
10	If (Time is averge) and (Celltemeprature is low) and (solarradiation is low) then (Thermalefficiecny is out1mf10) (1)
11	If (Time is averge) and (Celltemeprature is low) and (solarradiation is average) then (Thermalefficiecny is out1mf11) (1)
12	If (Time is averge) and (Celltemeprature is low) and (solarradiation is high) then (Thermalefficiecny is out1mf12) (1)
13	If (Time is averge) and (Celltemeprature is average) and (solarradiation is low) then (Thermalefficiecny is out1mf13) (1)
14	If (Time is averge) and (Celltemeprature is average) and (solarradiation is average) then (Thermalefficiecny is out1mf14) (1)
15	If (Time is averge) and (Celltemeprature is average) and (solarradiation is high) then (Thermalefficiecny is out1mf15) (1)
16	If (Time is averge) and (Celltemeprature is High) and (solarradiation is low) then (Thermalefficiecny is out1mf16) (1)
17	If (Time is averge) and (Celltemeprature is High) and (solarradiation is average) then (Thermalefficiecny is out1mf17) (1)
18	If (Time is averge) and (Celltemeprature is High) and (solarradiation is high) then (Thermalefficiecny is out1mf18) (1)
19	If (Time is High) and (Celltemeprature is low) and (solarradiation is low) then (Thermalefficiecny is out1mf19) (1)
20	If (Time is High) and (Celltemeprature is low) and (solarradiation is average) then (Thermalefficiecny is out1mf20) (1)
21	If (Time is High) and (Celltemeprature is low) and (solarradiation is high) then (Thermalefficiecny is out1mf21) (1)
22	If (Time is High) and (Celltemeprature is average) and (solarradiation is low) then (Thermalefficiecny is out1mf22) (1)
23	If (Time is High) and (Celltemeprature is average) and (solarradiation is average) then (Thermalefficiecny is out1mf23) (1)
24	If (Time is High) and (Celltemeprature is average) and (solarradiation is high) then (Thermalefficiecny is out1mf24) (1)
25	If (Time is High) and (Celltemeprature is High) and (solarradiation is low) then (Thermalefficiecny is out1mf25) (1)
26	If (Time is High) and (Celltemeprature is High) and (solarradiation is average) then (Thermalefficiecny is out1mf26) (1)
27	If (Time is High) and (Celltemeprature is High) and (solarradiation is high) then (Thermalefficiecny is out1mf27) (1)

and solar radiation are considered as inputs and thermal efficiency is considered as output. Based on the literature, Gaussian membership function gives the least prediction error. Therefore, the same function is used as membership function in this research.

Membership functions are applied to the input data and convert into linguistic variables in first layer (Fuzzification layer). Based on the Fuzzy Inference system (FIS) the rules are created in the second layer (Rule layer). Third layer is also called as normalization layer. In this layer, the weight values are normalized and calculates the strength of ith rule to the sum of strength of all rules. The defuzzification process takes place to convert the fussy results into numerical values in fourth layer (defussification layer). In fifth layer (Sum layer), the overall output is computed by summing all the incoming signals.

6.1. Results of ANFIS

The results of experimental study is discussed in the previous section. In order to reduce the time, cost and identify the relation between the inputs and output, prediction model has been developed using ANFIS in Matlab toolbox. For this purpose, the current work considers three inputs

(time, Cell temperature and solar radiation) and 1 output (Thermal efficiency) in this study. Initially, the experimental data have been split into three data sets namely training (60%), checking (15%) and test (25%). Then the membership function with three linguistic variables such as low, average, high are applied to the input data and shown in Figure 6. In order to obtain the results with less prediction error, the number iteration (epochs) was considered as 100. The loading of training and testing datasets into the ANFIS model is shown in Figures 7 and 8 respectively. From these figures, it is observed that the training and testing is carried out on 40 and 25 datasets respectively. The statistical data for both input and target data is given in Table 2. To predict the optimal results, the 27 linguistic rules have been considered and is given in Table 3.

6.2. ANFIS results and discussion

The root Mean Square Error (RMSE) and coefficient of determination (R^2) are used to determine the accuracy of the ANFIS model. These values can be determined by using Eqs. (9) and (10) also the percentage mean relative error can be computed by using Eq. (11).
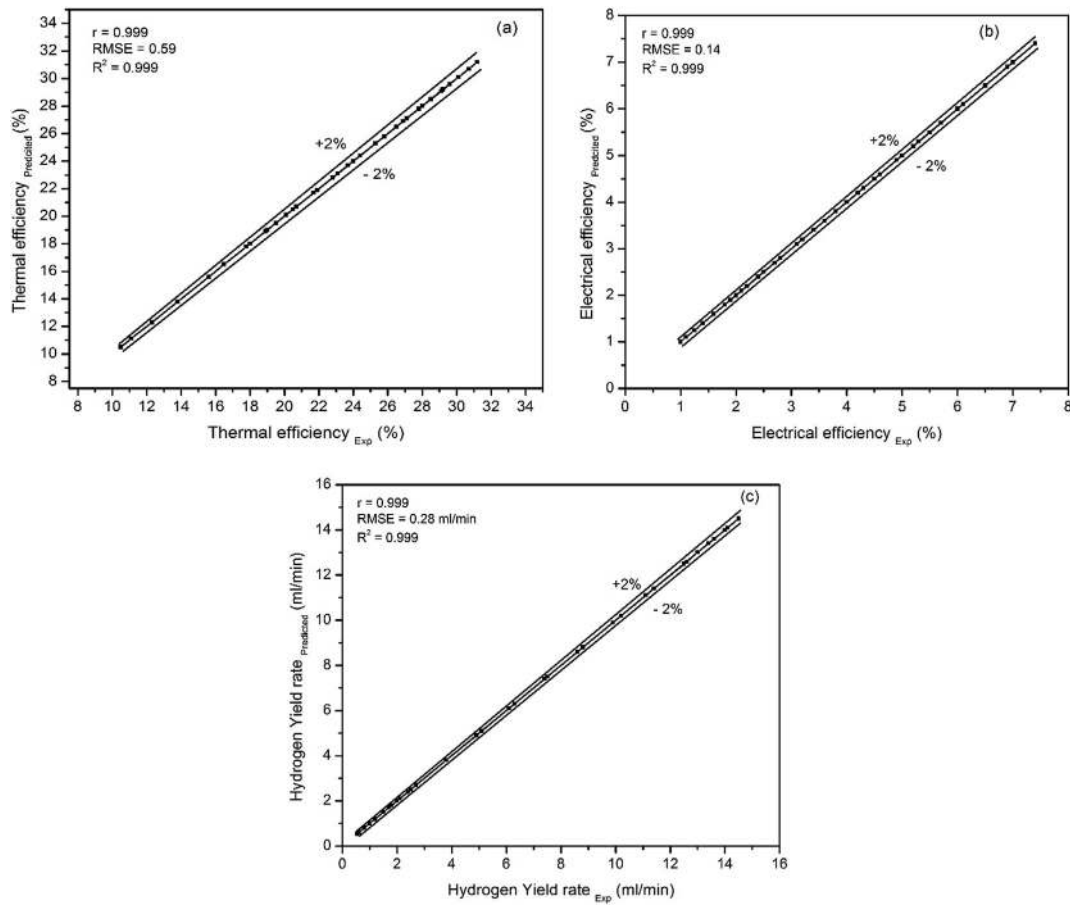
Figure 9. Comparison of the experimental values with the predicted values: (a) thermal efficiency (b) Electrical efficiency (c) Hydrogen yield rate.

Table 4. Results of ANFIS Model in Training and Testing datasets.

	Thermal Efficiency		Electrical Efficiency		Hydrogen Yield rate	
	Training	Testing	Training	Testing	Training	Testing
RMSE	0.00591	0.00655	0.00149	0.00167	0.00285	0.00337
R^2	0.99996	0.99984	0.00964	0.99977	0.99979	0.99980
R	0.99998	0.99992	0.09820	0.99989	0.99989	0.99990
MRE (%)	0.018	0.024	0.023	0.030	0.054	0.078

$$RMSE = \sqrt{\frac{1}{N}\sum_{x=1}^{N}(a_x - p_x)} \tag{9}$$

$$R^2 = \frac{\sum_{x=1}^{N}(a_x - p_x)}{\sum_{x=1}^{N}(a_x - a_x)} \tag{10}$$

$$MRE\ (\%) = \frac{1}{N}\sum_{x=1}^{N}\left[100\frac{|a_x - p_x|}{a_x}\right] \tag{11}$$

Where 'a_x' is the actual value, 'p_x' is the predicted value, '$\hat{a}_x$' is the mean of experimental value and 'N' is the total number of experiments.

The output values of the thermal efficiency, electrical efficiency and hydrogen yield rate is predicted by using ANFIS model is illustrated in Figure 9 (a) – (c) respectively. The predicted values are compared with the actual values by calculating the mean squared error (MSE), Mean Relative error (MRE) and R – square coefficient (R^2). The scattered diagrams are plotted by considering predicted values on the 'Y' axis and the actual values on the 'X' axis. Based upon the results obtained in ANFIS model, it can be clearly understood that, all the predicted values are close to the experimental values and the maximum error between the actual value and the predicted value is ±5%. The results of ANFIS model train and test stage are given in Table 4.

As indicated in Figure 9 (a), the ANFIS model for thermal efficiency gives a RMSE, R, R^2 and MRE of 0.61, 0.999, 0.999 and 0.018% respectively with the actual experimental values. This shows that the predicted values are very close to the experimental values and the ANFIS model predicts the values excellently. Similarly, the comparison between the predicted values and experimental values for electrical efficiency is shown in Figure 9 (b). The values of RMSE, R, R^2 and MRE of 0.14%, 0.999, 0.999 and 0.023% respectively are obtained for the electrical efficiency. It was is obvious to see that, the predicted values are very close agreement with the experimental values. In general, the hydrogen yield rate is mainly depends on thermal and electrical efficiency of the PVT system. The variation of predicted hydrogen yield rate with respect to the experimental value is given in Figure 9 (c). As expected, peak hydrogen

yield rate is obtained, when the PVT is placed at 40° inclination angle with respect to the ground. The same trend of results are also predicted in ANFIS model. Based on the prediction values, RMSE, R, R^2 and MRE of 0.28%, 0.999, 0.999 and 0.054% have been obtained. This shows that the testing data are in good agreement with training data.

7. Conclusions

In this study, the effect of PV module tilt angle, shape of thermal collector and the type of heat transfer fluid on the thermal efficiency, electrical efficiency and the hydrogen yield rate have been studied experimentally. Also the ANFIS model has been developed to predict the performance of PVT system and hydrogen yield rate. During this study, the following inferences are drawn.

1. The performance of the PVT system are measured by placing the PVT module at three different inclination angles (i.e. 30°, 40° and 50°). When PVT with spiral flow collector at 40° inclination angle, the thermal efficiency, electrical efficiency and hydrogen yield rate are 33.8%, 8.5% and 14.15 ml/min, which higher than that of 30° and 50° inclination angle respectively.
2. Adding spiral flow thermal collector with the PV module, the thermal efficiency, electrical efficiency and hydrogen yield rate of PVT system with water increased by 8.8%, 17.6% and 15% respectively compared with oscillatory flow thermal collector.
3. Compared with Ethylene Glycol based PVT system, thermal collector with water cooled the PV module efficiently. Therefore, the water based PVT system produce more hydrogen compared with other systems.
4. From these prediction results, it is concluded that the type of membership function, rules and number of inputs are mainly affects the ANFIS prediction results.
5. The ANFIS results revealed that the predicted values are in good agreement with the experimental values and it could be a suitable alternate method to predict the values of PVT systems in future.

Declarations

Author contribution statement

S. Senthilraja, R. Gangadevi, Hasan Köten & R. Marimuthu: Conceived and designed the experiments; Performed the experiments; Analyzed and interpreted the data; Contributed reagents, materials, analysis tools or data; Wrote the paper.

Funding statement

This research did not receive any specific grant from funding agencies in the public, commercial, or not-for-profit sectors.

Competing interest statement

The authors declare no conflict of interest.

Additional information

No additional information is available for this paper.

References

Ahmadi, P., Kjeang, E., 2015. Comparative life cycle assessment of hydrogen fuel cell passenger vehicles in different Canadian provinces. Int. J. Hydrogen Energy 40 (38), 12905–12917.

Ambrose, A.F., Al-Amin, A.Q., Rasiah, R., Saidur, R., Amin, N., 2017. Prospects for introducing hydrogen fuel cell vehicles in Malaysia. Int. J. Hydrogen Energy 42 (14), 9125–9134.

Aste, N., Del Pero, C., Leonforte, F., 2017. Water PVT collectors performance comparison. Energy Procedia 105, 961–966.

Aste, N., Leonforte, F., Del Pero, C., 2015. Design, modeling and performance monitoring of a photovoltaic–thermal (PVT) water collector. Sol. Energy 112, 85–99.

Awolusi, T.F., Oke, O.L., Akinkurolere, O.O., Sojobi, A.O., Aluko, O.G., 2019. Performance comparison of neural network training algorithms in the modeling properties of steel fiber reinforced concrete. Heliyon 5 (1), e01115.

Balthasar, W., 1984. Hydrogen production and technology: today, tomorrow and beyond. Int. J. Hydrogen Energy 9 (8), 649–668.

Bamberger, C.E., Richardson, D.M., 1976. Hydrogen production from water by thermochemical cycles. Cryogenics 16 (4), 197–208.

Bambrook, S.M., Sproul, A.B., 2016. A solvable thermal circuit for modelling PVT air collectors. Sol. Energy 138, 77–87.

Batayneh, W., Abdulhay, E., Alothman, M., 2020. Prediction of the performance of artificial neural networks in mapping sEMG to finger joint angles via signal pre-investigation techniques. Heliyon 6 (4), e03669.

Bhattacharyya, R., Misra, A., Sandeep, K.C., 2017. Photovoltaic solar energy conversion for hydrogen production by alkaline water electrolysis: conceptual design and analysis. Energy Convers. Manag. 133, 1–13.

Bracamonte, J., Parada, J., Dimas, J., Baritto, M., 2015. Effect of the collector tilt angle on thermal efficiency and stratification of passive water in glass evacuated tube solar water heater. Appl. Energy 155, 648–659.

Brown, J., 1994. Neural Fuzzy Adaptive Modelling and Control. Engelwood Cliffs. In: Harris, C. (Ed.).

Chen, H.L., Lee, H.M., Chen, S.H., Chao, Y., Chang, M.B., 2008. Review of plasma catalysis on hydrocarbon reforming for hydrogen production—interaction, integration, and prospects. Appl. Catal. B Environ. 85 (1-2), 1–9.

Chi, J., Yu, H., 2018. Water electrolysis based on renewable energy for hydrogen production. Chin. J. Catal. 39 (3), 390–394.

Dahbi, S., Aboutni, R., Aziz, A., Benazzi, N., Elhafyani, M., Kassmi, K., 2016. Optimised hydrogen production by a photovoltaic-electrolysis system DC/DC converter and water flow controller. Int. J. Hydrogen Energy 41 (45), 20858–20866.

Ersöz, A., 2008. Investigation of hydrocarbon reforming processes for micro-cogeneration systems. Int. J. Hydrogen Energy 33 (23), 7084–7094.

Farshchimonfared, M., Bilbao, J.I., Sproul, A.B., 2015. Channel depth, air mass flow rate and air distribution duct diameter optimization of photovoltaic thermal (PV/T) air collectors linked to residential buildings. Renew. Energy 76, 27–35.

Fudholi, A., Zohri, M., Rukman, N.S.B., Nazri, N.S., Mustapha, M., Yen, C.H., Mohammad, M., Sopian, K., 2019. Exergy and sustainability index of photovoltaic thermal (PVT) air collector: a theoretical and experimental study. Renew. Sustain. Energy Rev. 100, 44–51.

Gadalla, M., Zafar, S., 2016. Analysis of a hydrogen fuel cell-PV power system for small UAV. Int. J. Hydrogen Energy 41 (15), 6422–6432.

Gökmen, N., Hu, W., Hou, P., Chen, Z., Sera, D., Spataru, S., 2016. Investigation of wind speed cooling effect on PV panels in windy locations, 90. Renewable Energy, pp. 283–290.

Hegazy, A.A., 2000. Comparative study of the performances of four photovoltaic/thermal solar air collectors. Energy Convers. Manag. 41 (8), 861–881.

Hites, R.A., 2006. Persistent organic pollutants in the Great Lakes: an overview. Persistent Organic Pollutants in the Great Lakes. Springer, Berlin, Heidelberg, pp. 1–12.

Jain, D., Lalwani, M., 2017. A review on optimal inclination angles for solar arrays. Int. J. Renew. Energy Resour. 7 (3), 1053–1061.

Jang, J.S., Sun, C.T., 1995. Neuro-fuzzy modeling and control. Proc. IEEE 83 (3), 378–406.

Jia, J., Seitz, L.C., Benck, J.D., Huo, Y., Chen, Y., Ng, J.W.D., Bilir, T., Harris, J.S., Jaramillo, T.F., 2016. Solar water splitting by photovoltaic-electrolysis with a solar-to-hydrogen efficiency over 30%. Nat. Commun. 7 (1), 1–6.

Larsson, M., Mohseni, F., Wallmark, C., Grönkvist, S., Alvfors, P., 2015. Energy system analysis of the implications of hydrogen fuel cell vehicles in the Swedish road transport system. Int. J. Hydrogen Energy 40 (35), 11722–11729.

Le Roux, W.G., 2016. Optimum tilt and azimuth angles for fixed solar collectors in South Africa using measured data. Renew. Energy 96, 603–612.

Li, R., 2017. Latest progress in hydrogen production from solar water splitting via photocatalysis, photoelectrochemical, and photovoltaic-photoelectrochemical solutions. Chin. J. Catal. 38 (1), 5–12.

Lipman, T.E., Elke, M., Lidicker, J., 2018. Hydrogen fuel cell electric vehicle performance and user-response assessment: results of an extended driver study. Int. J. Hydrogen Energy 43 (27), 12442–12454.

Lu, H., Zhao, W., 2018. Effects of particle sizes and tilt angles on dust deposition characteristics of a ground-mounted solar photovoltaic system. Appl. Energy 220, 514–526.

Myhan, R., Bieranowski, J., Szwejkowski, Z., Sitnik, E., 2017. The effect of local meteorological conditions on the optimal tilt angle of a solar energy collector—a case study in Poland. J. Sol. Energy Eng. 139 (4).

Rawat, P., Dhiran, T.S., 2017. Comparative analysis of solar photovoltaic thermal (PVT) water and solar photovoltaic thermal (PVT) air systems. Int. J. Civil Mech. Energy Sci. 3 (1), 8–12.

Rivera-Niquepa, J.D., De Oliveira-De Jesus, P.M., Castro-Galeano, J.C., Hernández-Torres, D., 2020. Planning stand-alone electricity generation systems, a multiple objective optimization and fuzzy decision making approach. Heliyon 6 (3), e03534.

Rossmeisl, J., Logadottir, A., Nørskov, J.K., 2005. Electrolysis of water on (oxidized) metal surfaces. Chem. Phys. 319 (1-3), 178–184.

Samara, S., Natsheh, E., 2018. Modeling the output power of heterogeneous photovoltaic panels based on artificial neural networks using low cost microcontrollers. Heliyon 4 (11), e00972.

Tiwari, G.N., Fischer, O., Mishra, R.K., Al-Helal, I.M., 2016. Performance evaluation of N-photovoltaic thermal (PVT) water collectors partially covered by photovoltaic module connected in series: an experimental study. Sol. Energy 134, 302–313.

Tiwari, S., Agrawal, S., Tiwari, G.N., 2018. PVT air collector integrated greenhouse dryers. Renew. Sustain. Energy Rev. 90, 142–159.

Touafek, K., Khelifa, A., Haloui, H., El Hocine, H.B.C., Boutina, L., Baissi, M.T., Haddad, S., Tabet, I., Malek, A., 2018. December. Improvement of performances of solar photovoltaic/thermal air collector in South Algeria. In: 2018 6th International Renewable and Sustainable Energy Conference (IRSEC). IEEE, pp. 1–5.

Yazdanpanahi, J., Sarhaddi, F., Adeli, M.M., 2015. Experimental investigation of exergy efficiency of a solar photovoltaic thermal (PVT) water collector based on exergy losses. Sol. Energy 118, 197–208.